NUCLEAR THEORY, Vol. 42 (2025)
eds. M. Gaidarov, N. Minkov, Heron Press, Sofia

Spontaneous Fission, Cluster Radioactivity and Alpha Decay from Ground and K-Isomeric States of Heavy and Superheavy Nuclei within Cluster Approach

I.S. Rogov[1,2], **G.G. Adamian**[1], **N.V. Antonenko**[1,2]

[1]Joint Institute for Nuclear Research, 141980 Dubna, Russia
[2]Tomsk Polytechnic University, 634050 Tomsk, Russia

Abstract. The spontaneous fission, cluster radioactivity and alpha-decay processes are studied within the dinuclear system model. All these processes are considered as the evolution of a nucleus in the charge (mass) asymmetry coordinate. For the even-even and even-odd actinides and superheavy nuclei, the spontaneous fission and alpha-decay half-lives of the ground and K-isomeric states are calculated and compared with the existing experimental data. The mechanism of the spontaneous fission hindrance of the high-K ground and isomeric states is explained.

1 Introduction

Alpha-decay (AD), cluster radioactivity (CR) and spontaneous fission (SF) attract attention in connection with the studies of the structure of heavy and superheavy nuclei. One of the most challenging tasks is to describe the AD, SF and CR processes in a single approach with the same Hamiltonian. While the SF results in the products with masses close to the half of the mass of mother nucleus, the CR and AD produce quite asymmetric fragments. So the AD and CR can be considered as the super-asymmetric fission. An intriguing question is whether this approach is good for the K-isomeric states as well as for the ground state of even-even and even-odd nuclei. The longer half-life of the isomeric state compared to the ground state suggests that there is substantial fission hindrance (FH) because of the large value of K. Experimental and theoretical studies of this issue continue to be of interest for assessing the survival of superheavy nuclei (SHN).

2 Model

Fission process is considered here within the dinuclear system (DNS) model [1–4] in which the formation of cluster with charge number $Z_L \geq 2$ is described as the evolution of the system in charge asymmetry coordinate $\eta_Z = (Z_H - Z_L)/(Z_H + Z_L)$. Here, Z_i (A_i), where $i = L, H$, is the charge (mass) number

of the i-th cluster and $Z = Z_L + Z_H$ ($A = A_L + A_H$) is the total charge (mass) number of the DNS. The $\eta_Z = 1$ corresponds to the state of mononucleus (clusterless nucleus), and $\eta_Z = 0$ is for the symmetric DNS configuration. The mass asymmetry coordinate $\eta = (A_H - A_L)/A$ is assumed to be strongly related to η_Z by the condition of the potential energy minimum. Indeed, at given η_Z the DNS potential energy as a function of η has a well-defined minimum. So, the spreading in η is small at each η_Z. The decay of the formed DNS is considered as a motion of the DNS in the relative distance R.

Thus, the probability of finding two clusters L and H at given η_Z is proportional to the leakage of the ground-state wave function in R at this η_Z. To simplify the description of cluster decay, the process is usually divided into two independent stages: forming the cluster state or DNS, and its decay in R coordinate [5].

The probability of DNS formation (spectroscopic factor) S_L is determined by solving the stationary Schrödinger equation [1–4]

$$H\Psi_n(\eta_Z) = E_n\Psi_n(\eta_Z), \tag{1}$$

where the collective Hamiltonian

$$H = -\frac{\hbar^2}{2}\frac{\partial}{\partial\eta_Z}\left(B^{-1}\right)_{\eta_Z}\frac{\partial}{\partial\eta_Z} + U(R_m, \eta_Z, \Omega) \tag{2}$$

contains the inverse inertia coefficient $\left(B^{-1}\right)_{\eta_Z}$ [6] and the potential energy U [7] calculated at the touching distance $R = R_m$ at given η_Z. The model presented here belongs to the cluster type, because the ground state of the nucleus is assumed to have a small admixture of cluster-state components. Here the cluster state means two touching nuclei or a DNS. The total wave function $\Psi_n(\eta_Z)$ of the nucleus is expressed by a superposition of cluster and clusterless components. Since we assume that the spin and parity of the fissioning nucleus are preserved during SF, all cluster and clusterless components have the same spin and parity as in the parent nucleus. These effects are effectively described through the inclusion of the centrifugal potential in the DNS potential energy [7]

$$U(R_m, \eta_Z, \Omega) = V(R_m, \eta_Z, \Omega) + (Q_L + Q_H - Q_M), \tag{3}$$

which, as a function of charge asymmetry, is referred to a driving potential. Here, Q_M and $Q_{L,H}$ are the experimental mass excesses [8] of the parent nucleus and the nuclei forming the DNS, respectively. If the experimental mass excesses are not available, we take the theoretical values from Refs. [9–11]. The energy of isomeric state is taken into account in Q_M. The pecularities of structure of the DNS nuclei are taken into account through $Q_{L,H}$. The tip-tip orientation of axial symmetric deformed nuclei is taken in the calculations of driving potentials because it provides the minimum of the potential energy of the DNS considered.

The nucleus-nucleus interaction potential

$$V(R, \eta_Z, \Omega) = V_{\rm C}(R, \eta_Z) + V_N(R, \eta_Z) + V_r(R, \eta_Z, \Omega) \tag{4}$$

in (3) consists of the Coulomb $V_{\rm C}$, nuclear V_N, and centrifugal V_r parts. The nuclear part V_N of the interaction potential is calculated in the double folding form, where the density-dependent nucleon-nucleon forces are folded with the nucleon densities of heavy and light nuclei of the DNS [1–4]. The centrifugal potential is calculated as

$$V_r = \hbar^2\Omega(\Omega+1)/(2\Im)\,, \tag{5}$$

where Ω is the spin of fissioning nucleus and $\Im = c_1(\Im_L + \Im_H + \mu R_m^2)$ is the moment of inertia of the DNS ($\Im_{L,H}$ are rigid body moments of inertia for the clusters of the DNS, $c_1 = 0.85$ for all considered fissioning nuclei [5, 12, 13], and $\mu = m_0 A_L A_H/A$ is the reduced mass parameter (m_0 is the nucleon mass)). Note that the nucleus-nucleus potential depends on the ground-state quadrupole deformations [14] of the DNS nuclei and has a minimum at $R = R_m(\eta_Z, \Omega)$ [1–4].

The driving potential for the fissioning nucleus ^{258}No is shown in Figure 1. The values of U and $\left(B^{-1}\right)_{\eta_Z}$ are extended to the segments of the width $2\Delta = 2/Z$ so that the points η_Z are placed in the middle of the corresponding segments. The only exception is the mononucleus, for which we set $\eta_Z \in (1 - 4\Delta, 1]$ and the α-particle DNS with $\eta_Z \in (1 - 5\Delta, 1 - 4\Delta]$. The SF mainly occurs from the DNS configurations corresponding to the minima of the driving potential with energies smaller than the ground-state energy [1–4], i.e., at about $1 - \eta_Z > 0.6$. To undergo SF through the energy-resolved region with the

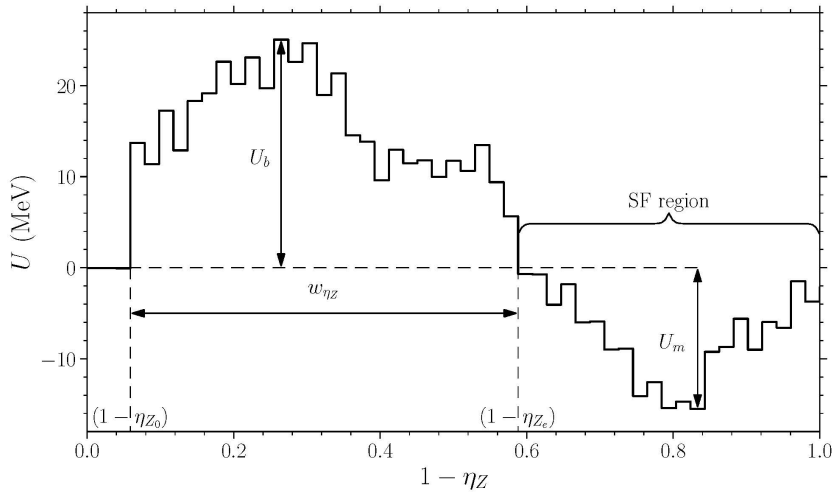

Figure 1. Driving potential for ^{258}No. The fission barrier in η_Z is characterized by the height U_b and the width w_{η_Z}. The depth of the global potential minimum in the SF region is denoted by U_m. The tip-tip orientation of nuclei is taken in the DNS.

global potential minimum of the depth U_m at $\eta_Z \approx 0.2$, the fissioning nucleus should penetrate the barrier of height U_b and width w_{η_Z} (Figure 1). The values $1-\eta_{Z_0}$ and $1-\eta_{Z_e}$ are the entrance and exit turning points, respectively. Note that SF events occurs also from the sub-barrier region but their contributions are negligible compared to the contributions from the energy-resolved region.

The preformation probability S_L of the DNS with certain charge number Z_L of light cluster is defined as

$$S_L = \int\limits_{\eta_Z(Z_L)-\Delta}^{\eta_Z(Z_L)+\Delta} |\Psi(\eta_Z)|^2 d\eta_Z. \tag{6}$$

For the AD and CR in the potential barrier region at about $1-\eta_Z \leq 0.6$ (Figure 1), the half-life is calculated as

$$T_{1/2}^{\alpha,\mathrm{cl}} = \frac{\hbar \ln 2}{\Gamma_L} = \frac{\pi \ln 2}{\omega_0 S_L P_L}, \tag{7}$$

where Γ_L is the decay width and P_L is the penetration probability of the α-particle or cluster through the Coulomb barrier calculated in the WKB approach [1–4]. The value of frequency ω_0 of zero-point vibration in η_Z coordinate near the mononucleus state ($\eta_Z \approx 1$) is equal to the distance between the ground and the first excited state of DNS vibrating in η_Z. In the case of SF, all DNS configurations in the SF region contribute because their decay probabilities P_L in R coordinate are equal to 1. Therefore, the SF half-life is calculated as

$$T_{1/2}^{\mathrm{sf}} = \frac{\pi \ln 2}{\omega_0 S_{\mathrm{sf}}}, \tag{8}$$

where

$$S_{\mathrm{sf}} = \int\limits_{0}^{\eta_{Z_e}} |\Psi(\eta_Z)|^2 d\eta_Z \tag{9}$$

and η_{Z_e} is the exit turning point (see Figure 1).

3 SF, CR and AD from Ground State of Actinides

To verify the model, the half-lives with respect to AD, CR, and SF are calculated (Table 1 – 3) and compared with the experimental data [15] for even uranium

Table 1. Calculated $T_{1/2}^{\alpha}$(th.) and experimental $T_{1/2}^{\alpha}$(exp.) α-decay half-lives (in units of s) for even-even U isotopic chain

	^{232}U	^{234}U	^{236}U
$T_{1/2}^{\alpha}$(th.)	3.021×10^{9}	9.15×10^{12}	9.49×10^{15}
$T_{1/2}^{\alpha}$(exp.)	3.20×10^{9}	7.74×10^{12}	1.00×10^{15}

Table 2. The same as in Table 1, but for CR half-lives

	$^{232}\mathrm{U} \to {}^{24}\mathrm{Ne}$	$^{234}\mathrm{U} \to {}^{26}\mathrm{Ne}$	$^{234}\mathrm{U} \to {}^{28}\mathrm{Mg}$	$^{236}\mathrm{U} \to {}^{30}\mathrm{Mg}$
$T^{\mathrm{cl}}_{1/2}$(th.)	4.07×10^{21}	1.29×10^{25}	4.33×10^{25}	1.85×10^{26}
$T^{\mathrm{cl}}_{1/2}$(exp.)	1.89×10^{21}	1.20×10^{25}	3.47×10^{25}	1.89×10^{26}

Table 3. The same as in Table 1, but for SF half-lives

	^{232}U	^{234}U	^{236}U
$T^{\mathrm{sf}}_{1/2}$(th.)	7.43×10^{20}	1.61×10^{22}	1.10×10^{23}
$T^{\mathrm{sf}}_{1/2}$(exp.)	3.73×10^{21}	4.73×10^{23}	6.38×10^{23}

isotopes ^{232,234,236}U. Here, we consider only the decays of even-even nuclei from their ground states. A good agreement between the theory and experiment has been obtained. The maximal deviation from the experimental half-lives is within the factor of 6 that is rather good in the present case without special adjustment of the parameters. Simultaneous good description of the AD, CR and SF in ^{232,234,236}U allows us to apply the model to the nuclei ^{236,238}Pu and ^{242}Cm (Table 4 – 6). As seen in Tables 4 – 6, the description of AD and CR is pretty good. The emission half-lives of neighboring clusters ^{28}Mg($T^{\mathrm{cl}}_{1/2}$ =

Table 4. Calculated $T^{\alpha,\mathrm{cl},\mathrm{sf}}_{1/2}$(th.) and experimental $T^{\alpha,\mathrm{cl},\mathrm{sf}}_{1/2}$(exp.) α-decay, CR, and SF half-lives (in units of s) for ^{236}Pu

	^{4}He	^{28}Mg	SF
$T^{\alpha,\mathrm{cl},\mathrm{sf}}_{1/2}$(th.)	4.80×10^{8}	2.06×10^{21}	4.24×10^{17}
$T^{\alpha,\mathrm{cl},\mathrm{sf}}_{1/2}$(exp.)	1.30×10^{8}	4.67×10^{21}	1.10×10^{17}

Table 5. The same as in Table 4, but for for ^{238}Pu

	^{4}He	^{30}Mg	^{23}Si	SF
$T^{\alpha,\mathrm{cl},\mathrm{sf}}_{1/2}$(th.)	1.21×10^{9}	2.79×10^{25}	5.15×10^{25}	1.01×10^{19}
$T^{\alpha,\mathrm{cl},\mathrm{sf}}_{1/2}$(exp.)	3.90×10^{9}	5.01×10^{25}	1.99×10^{25}	1.26×10^{18}

Table 6. The same as in Table 4, but for ^{242}Cm

	^{4}He	^{34}Si	SF
$T^{\alpha,\mathrm{cl},\mathrm{sf}}_{1/2}$(th.)	3.49×10^{7}	2.09×10^{23}	2.53×10^{14}
$T^{\alpha,\mathrm{cl},\mathrm{sf}}_{1/2}$(exp.)	1.90×10^{7}	1.41×10^{23}	2.32×10^{14}

3.18×10^{25} s) and ^{30}Mg($T^{\rm cl}_{1/2} = 2.79 \times 10^{25}$ s) from ^{238}Pu are predicted. The SF mainly occurs from the DNS configurations corresponding to the minima of the driving potentials at $Z_L = 38 - 42$. The potential energies of these minima are smaller than the potential energy of mother nucleus. The wave function in η_Z has local maxima in these potential minima. As known, the U, Pu, and Cm isotopes considered have asymmetric mass distributions of fragments of the SF. The life-time with respect to the SF is also well described for most of the nuclei.

Besides the good description of half-lives with respect to α-decay and SF for ^{248}Cf, we predict CR with the emission of ^{40}S in this nucleus (see Table 7). This is possible candidate for future experiment, which has has a half-life to be measurable with present experimental setups and reasonable branching ratio with respect to α-decay. For the comparison, $T^{\rm cl}_{1/2}(^{248}{\rm Cf} \rightarrow^{40} {\rm S}) = 233$ s, $T^{\rm cl}_{1/2}(^{242}{\rm Cm} \rightarrow^{34} {\rm Si}) = 4.88 \times 10^{25}$ s, $T^{\rm cl}_{1/2}(^{248}{\rm Cf} \rightarrow^{46} {\rm Ar}) = 3.28 \times 10^{26}$ s, and $T^{\rm cl}_{1/2}(^{248}{\rm Cf} \rightarrow^{50} {\rm Ca}) = 2.63 \times 10^{28}$ s.

Table 7. The same as in Table 4, but for ^{248}Cf

	^{4}He	^{40}S	SF
$T^{\alpha,{\rm cl},{\rm sf}}_{1/2}$(th.)	3.16×10^{7}	4.88×10^{25}	1.96×10^{12}
$T^{\alpha,{\rm cl},{\rm sf}}_{1/2}$(exp.)		1.29×10^{12}	

4 Isotopic Trends of SF and AD

The calculated SF and AD half-lives $T_{1/2}$ of the even isotopes of U, Pu, Cm, Cf, Fm, No, Rf, Sg, and Hs are presented in Figure 2. As seen, the theoretical results are in quite a good agreement with the experimental data. For the SF (AD) of ^{232}Th, $T_{1/2} = 1.75 \times 10^{28}$ s ($T_{1/2} = 3.73 \times 10^{17}$ s), while the experimental half-life is $T_{1/2} = 4 \times 10^{28}$ s ($T_{1/2} = 4.42 \times 10^{17}$ s). For the SF, the largest differences of about factor of 30 and 8 are for ^{234}U and ^{238}Pu, respectively. However, it is acceptable for the model without adjustment of the parameters which were set the same for all nuclei considered. The calculations reproduce the isotopic trends of $T_{1/2}$, the enhanced stability at $N = 152$ for Fm and No, and the rather weak dependence of $T_{1/2}$ on N at $N = 152$ for Rf and Sg. We predict long half-lives at $N = 164$ for Sg and Hs. The values of $T_{1/2}$ are almost comparable for ^{270}Hs ($N = 162$), ^{272}Hs ($N = 164$) and differ by less than 3 times for ^{268}Sg ($N = 162$) and ^{270}Sg ($N = 164$). The existing fission models predict the maximum of $T_{1/2}$ at $N = 162$. In our model, the absolute values of $T_{1/2}$ for the ^{268,270}Sg and ^{270,272}Hs nuclei to $N = 162$ is much orders of magnitude smaller than in the self-consistent fission models. Note that for Sg an Hs a stabilization against AD occurs at $N = 162$ (Figure 2).

We find that the influences of the shape of the potential barrier (i.e., the width) and the inertia parameter for the fission are significant, and therefore they

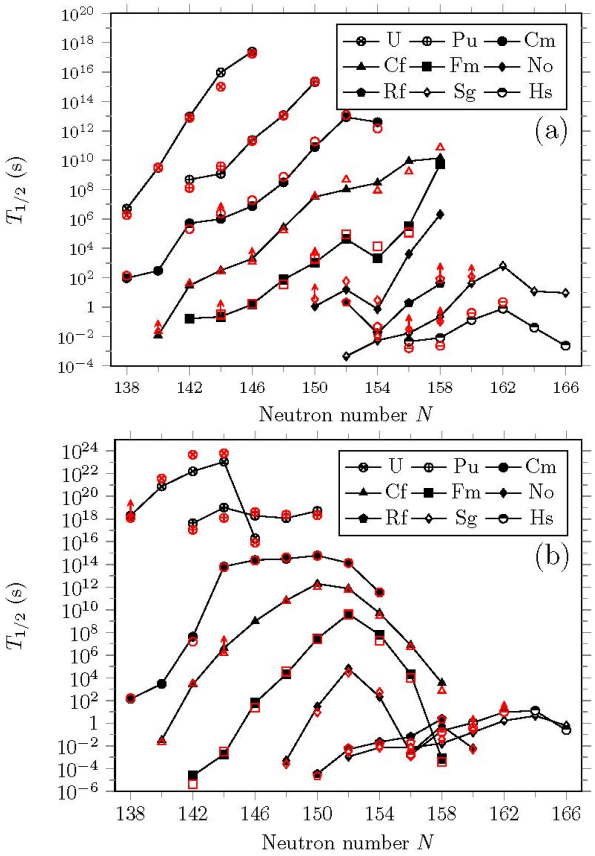

Figure 2. Calculated (symbols connected by lines) and experimental (red open symbols) [15] AD (a) and SF (b) half-lives $T_{1/2}$ of the even isotopes of U, Pu, Cm, Cf, Fm, No, Rf, Sg, and Hs. Arrows indicate the lower limit of half-lives.

are as important as the height of the barrier. Note that the height of the barriers in η_Z is much larger than the height of the barriers in macroscopic-microscopic and self-consistent mean-field fission models. Thus, the fission half-lives do not allow us to make an unambiguous conclusion about the height of the potential barriers, where the barrier appears along elongation of the fissioning nucleus.

5 Hindrance of SF and AD from Ground State of Even-Odd Nuclei

The calculated half-lives $T_{1/2}$ of even-odd and even-even nuclei are in a good agreement with the available experimental data for AD and SF (Figure 3). For the SF (AD) of ^{235}U, ^{239}Pu, and ^{241}Pu, $T_{1/2} = 1.65 \times 10^{26}$, 5.39×10^{23}, and 3.04×10^{24} s ($T_{1/2} = 6.49 \times 10^{16}$, 2.73×10^{11}, and 2.60×10^{13} s), while the

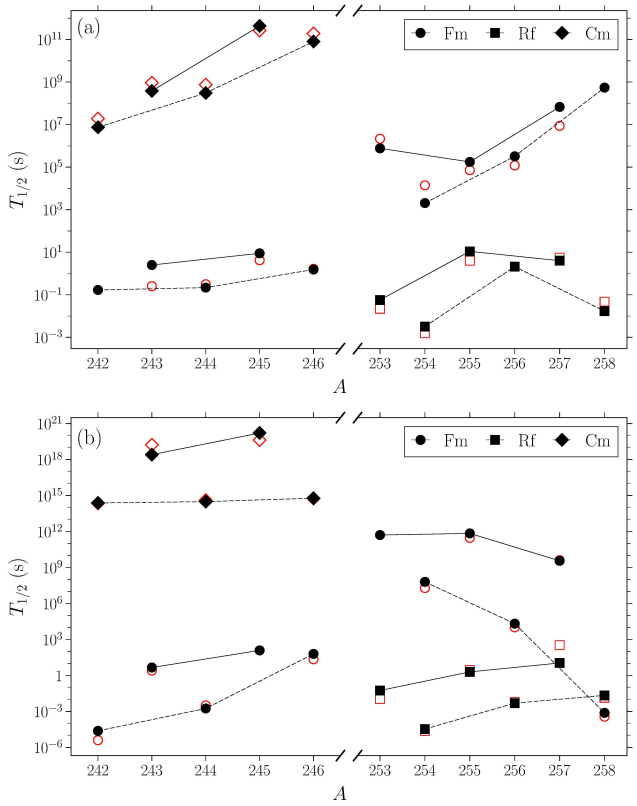

Figure 3. Calculated (black solid symbols) and experimental (red open symbols) [15] AD (a) and SF (b) half-lives $T_{1/2}$ for Cm, Fm, Rf isotopes. The even-odd (even-even) isotopes are connected with solid (dashed) lines to guide eyes.

experimental half-lives are $T_{1/2} = 3.19 \times 10^{26}$, 2.54×10^{23}, and $\approx 1.89 \times 10^{24}$ s ($T_{1/2} = 2.23 \times 10^{16}$, 7.61×10^{11}, and 4.52×10^{13} s), respectively. For the fissioning nuclei ^{235}U, ^{239}Pu, and ^{241}Pu, the measured FH are, respectively, 518, 1.1×10^5, and $\approx 6.7 \times 10^5$ [3]. Using the calculated $\Omega = 1/2$ from Ref. [16], we predict $T_{1/2} = 124$ s for the SF of ^{245}Fm. As seen in Figure 3, the AD and SF half-lives of even-odd isotopes are larger than expected geometrically mean half-lives of the neighboring even-even nuclei. This means that the odd-even effects of AD and SF half-lives are correctly included in the model. For the SF, the the rotational term of the driving potential is mainly responsible for this effect and, correspondingly, for the FH. The centrifugal potential strongly affects the shape of the driving potential in the region of asymmetric DNS, especially for the DNS with α-particle. It shifts the ground-state wave function towards the mononucleus configuration and strongly reduces the probabilities of the DNS

formation in the SF region with $1 - \eta_Z > 0.6$, and, correspondingly, affects the value of SF half-life. For the AD, the penetration probability P_L plays important role. The centrifugal potential increases the height of Coulomb barrier and, correspondingly, decreases P_L and $T_{1/2}$. For even-odd and neighboring even-even nuclei, the probabilities of α-particle formation do not differ much from each other.

6 SF and AD from K-Isomeric and Ground States

The K-isomeric states are characterized by two parameters: spin projection K and energy E. The value of spin $\Omega = K$ is taken directly into consideration in the rotational part (5) of the driving potential. The energy E of isomeric state is introduced as an addition to the mass excess Q_M of the parent nucleus in (3). The spin $\Omega = K$ and energy E of K-isomer modify both the shape and height of fission barrier in η_Z in comparison to the ground-state fission barrier and, correspondingly, change SF and AD half-lives.

In even-odd nuclei, the energies E of K-isomeric states are small ($\leq$ 200 keV for nuclei considered), therefore, the hindrance factors of SF from the K-isomeric and ground states have the same origin. With growing value of K, there is an increase in the half-life and vice versa.

In the case of even-even nuclei, the energies of K-isomeric states are much more "weighty" and are on the order of several MeV. In this case, the actions of the spin and energy on the isomer half-life are opposite. Non-zero value of K increases the driving potential, mainly in the area of the most asymmetric configurations. With growing $1 - \eta_Z$ the influence of $K \neq 0$ on the driving potential becomes less noticeable. The energy E of isomeric state affects the full driving potential, lowering it over the entire region of η_Z. Thus, the energy of isomeric state weakens the effect of the growth of the driving potential with spin and reduces the potential barrier in η_Z, as well as lowers the potential pocket in the region of SF. As a result, the effect of spin can be overcompensated by the effect of energy, which eventually leads to the fact that the SF from the K-isomeric state proceeds easier than from the ground state. Since the mass parameters for ground and isomeric states are close in magnitude, the role of mass parameter in the FH is weaker than the role of potential energy.

As seen in Tables 8 – 11, the calculated half-lives of even-even and even-odd nuclei are consistent with the available experimental data for SF and AD from the ground and isomeric states. It seems that theory is able to estimate unknown values of SF half-lives. The calculated results strongly depend on a nucleus considered. Since the value of $T^{\rm sf}_{1/2}$ of isomeric state decreases with increasing E, but increases with K, then for some E and K this $T^{\rm sf}_{1/2}$ can be smaller than the half-life of α-decay and closer to the value of half-life of the electromagnetic decay of the isomeric state. For example, as seen for the isomeric states of even isotopes of No, there is an increase of SF half-life with number of neutrons and $T^{\rm sf}_{1/2} < T^{\alpha}_{1/2}$ for the isomeric states of even-even nu-

Table 8. The calculated (th.) and experimental (exp.) AD ($T^{\alpha}_{1/2}$) half-lives for the ground states ($E = 0$) and K-isomers with the excitation energies E in even-even nuclei. The calculated spectroscopic factors S_{α} for the α-particle are also presented. The experimental data are either from Ref. [9] or indicated references

Nucleus	K^{π}	E (MeV)	S_{α}	$T^{\alpha}_{1/2}$(th.) (s)	$T^{\alpha}_{1/2}$(exp.) (s)
^{244}Cm	0^+	0	5.15×10^{-2}	3.06×10^{8}	7.50×10^{8}
	6^+	1.042	4.28×10^{-2}	1.05×10^{9}	
^{250}Fm	0^+	0	5.99×10^{-2}	1.06×10^{3}	2.00×10^{3}
	(8^-)	1.199	3.89×10^{-2}	3.39×10^{5}	
^{256}Fm	0^+	0	6.56×10^{-2}	3.23×10^{5}	1.20×10^{5}
	7^-	1.425	3.95×10^{-3}	6.23×10^{6}	
^{250}No	0^+	0	7.60×10^{-2}	1.85×10^{-3}	$> 2.1 \times 10^{-4}$
	(6^+)	1.050	6.14×10^{-3}	12.0	
	(16^+)	2.3	1.13×10^{-2}	6.4	
^{252}No	0^+	0	7.07×10^{-2}	15.8	56.7
	(8^-)	1.255	5.30×10^{-2}	2.18×10^{3}	
	(16^+)	2.7	7.72×10^{-2}	2.89×10^{2}	
^{254}No	0^+	0	6.50×10^{-2}	7.39×10^{-1}	2.93
	(8^-)	1.297	3.10×10^{-3}	7.84×10^{3}	2.80×10^{3}
	(16^+)	2.917	1.99×10^{-2}	1.47×10^{6}	
^{254}Rf	0^+	0	8.07×10^{-2}	3.22×10^{-2}	$> 1.55 \times 10^{-3}$
	(8^-)	1.10	5.77×10^{-2}	2.19×10^{2}	
	(16^+)	2.25	2.63×10^{-2}	5.38×10^{4}	
^{256}Rf	0^+	0	7.76×10^{-2}	2.11	2.08
	(7^-)	1.40	9.20×10^{-2}	8.46×10^{1}	
	(13^-)	2.42	8.74×10^{-2}	3.13	
^{262}Rf	(0^+)	0	9.00×10^{-2}	1.10	
	(8^-)	1.20	8.52×10^{-2}	1.91	

clei and, correspondingly, the SF and γ-transitions may be the main competing processes. For the isomeric states of even-odd nuclei, we have $T^{\alpha}_{1/2} < T^{sf}_{1/2}$ with only the one exception for ^{255}Rf, where $T^{\alpha}_{1/2}$ and $T^{sf}_{1/2}$ are comparable. In ^{254}No, there are isomers with K=8, E=1.297 MeV and K=16, E=2.917 MeV and the ratio $T^{sf}_{1/2}(K = 16)/T^{sf}_{1/2}(K = 8) \approx 6$ (Table 9). In the case of ^{254}Rf, where E=1.1 and 2.25 MeV at K=8 and 16, respectively, the ratio $T^{sf}_{1/2}(K = 16)/T^{sf}_{1/2}(K = 8) \approx 10^3$ (Table 9). The large difference between these ratios in ^{254}No and ^{254}Rf is due to the energy $\Delta E = E(K = 16) - E(K = 8)$ difference in both nuclei: $\Delta E \approx 1.60$ and 1.15 MeV in ^{254}No and ^{254}Rf, respectively. We

Table 9. Same as the Table 8, but for SF ($T^{\rm sf}_{1/2}$) half-lives

Nucleus	K^π	E (MeV)	S_α 10^{-2}	$T^{\rm sf}_{1/2}$(th.) (s)	$T^{\rm sf}_{1/2}$(exp.) (s)
^{244}Cm	0^+	0	5.15	3.13×10^{14}	4.17×10^{14}
	6^+	1.042	4.28	1.50×10^{9}	
^{250}Fm	0^+	0	5.99	2.86×10^{7}	2.52×10^{7}
	(8^-)	1.199	3.89	2.63×10^{4}	
^{256}Fm	0^+	0	6.56	2.10×10^{4}	1.04×10^{4}
	7^-	1.425	0.39	3.6×10^{-1}	$8^{+88}_{-7} \times 10^{-4}$ [17]
^{250}No	0^+	0	7.60	12.0×10^{-6}	$3.7^{+1.1}_{-0.8} \times 10^{-6}$ [18] $3.8^{+0.3}_{-0.3} \times 10^{-6}$ [19] $4.0^{+4}_{-4} \times 10^{-6}$ [20] 4.7×10^{-6} [21]
	(6^+)	1.050	0.61	22.0×10^{-6}	$43^{+22}_{-15} \times 10^{-6}$ [18] $> 34.9^{+3.9}_{-3.2} \times 10^{-6}$ [19] $> 40 \times 10^{-6}$ [20]
	(16^+)	2.3	1.13	1.3×10^{-6}	$\geq 0.7^{+1.4}_{-0.3} \times 10^{-6}$ [20]
^{252}No	0^+	0	7.07	29.4	9
	(8^-)	1.255	5.30	2.05×10^{-1}	
	(16^+)	2.7	7.72	1.71×10^{-4}	
^{254}No	0^+	0	6.50	6.55×10^{4}	2.88×10^{4}
	(8^-)	1.297	0.31	1.41×10^{3}	1.40×10^{3} $> 4.70 \times 10^{3}$ [22]
	(16^+)	2.917	1.99	8.36×10^{3}	≥ 1.65
^{254}Rf	0^+	0	8.07	3.45×10^{-5}	2.30×10^{-5}
	(8^-)	1.10	5.77	1.14×10^{-4}	$> 4.70 \times 10^{-5}$
	(16^+)	2.25	2.63	1.36×10^{-1}	$> 6.02 \times 10^{-4}$
^{256}Rf	0^+	0	7.76	4.98×10^{-3}	6.40×10^{-3}
	(7^-)	1.40	9.20	1.78×10^{-5}	$1.4^{+0.6}_{-0.4} \times 10^{-5}$ [23]
	(13^-)	2.42	8.74	1.29×10^{-6}	
^{262}Rf	(0^+)	0	9.00	6.61	≥ 2.30
	(8^-)	1.20	8.52	6.55×10^{-1}	2.50×10^{-1}

find that the SF half-life of the $K^\pi = 6^+$ isomer in ^{250}No is comparable with that of the ground state (within a factor of 2) and the half-life of the internal γ-transition to the ground state [19–21]. Because of this fact we are not able to distinguish whether the isomer decays via SF directly or proceeds through a K-forbidden electromagnetic decay to the ground state, which then goes to fission. The SF half-life of the second $K^\pi = 16^+$ isomer in ^{250}No is predicted about 1.5 μs. The isomeric states of ^{254}Rf are more stable against the SF than the ground

Table 10. The calculated (th.) and experimental (exp.) AD ($T^{\alpha}_{1/2}$) half-lives for the ground states ($E = 0$) and K-isomers with the excitation energies E in even-odd nuclei. The calculated spectroscopic factors S_{α} for the alpha particle are also presented. The experimental data are either from Ref. [9] or indicated references. The values of $T^{\rm sf}_{1/2}$(exp.) for ^{253}Rf are different in Refs. [25] and [26] because of different assignments of K to the ground and isomeric states

Nucleus	K^{π}	E (MeV)	S_{α}	$T^{\alpha}_{1/2}$(th.) (s)	$T^{\alpha}_{1/2}$(exp.) (s)
^{243}Cm	$\frac{5}{2}^+$	0	5.26×10^{-2}	3.81×10^{8}	9.21×10^{8}
	$\frac{1}{2}^+$	0.087	7.42×10^{-2}	1.30×10^{6}	
^{249}No	$\left(\frac{7}{2}^+\right)$	0	8.60×10^{-2}	3.14×10^{-2}	1.50×10^{-2}
	$\left(\frac{1}{2}^+\right)$	0.100	4.96×10^{-2}	3.41×10^{-3}	
^{251}No	$\left(\frac{7}{2}^+\right)$	0	7.14×10^{-2}	7.59	
	$\left(\frac{1}{2}^+\right)$	0.106	8.81×10^{-2}	1.31×10^{-1}	
^{255}No	$\left(\frac{1}{2}^+\right)$	0	3.33×10^{-2}	3.17×10^{2}	7.04×10^{2}
	$\left(\frac{11}{2}^+\right)$	0.270	4.29×10^{-2}	6.24×10^{5}	
	$\left(\frac{21}{2}^+\right)$	1.50	2.21×10^{-2}	3.12×10^{4}	
^{253}Rf	$\left(\frac{7}{2}^+\right)$	0	4.41×10^{-2}	0.84×10^{-2}	2.20×10^{-2}
	$\left(\frac{1}{2}^+\right)$	0			
	$\left(\frac{1}{2}^+\right)$	0.200	5.23×10^{-2}	4.1×10^{-3}	6.00×10^{-3}
	$\left(\frac{7}{2}^+\right)$	0.200			
^{255}Rf	$\left(\frac{7}{2}^+\right)$	0	6.91×10^{-2}	11	4
	$\left(\frac{1}{2}^+\right)$	0.140	4.07×10^{-2}	2.94×10^{-2}	
^{257}Rf	$\left(\frac{1}{2}^+\right)$	0	8.67×10^{-2}	1.24	5.55
	$\left(\frac{7}{2}^+\right)$	0.073	1.59×10^{-2}	21.90	5.40
	$\left(\frac{21}{2}^+\right)$	1.0832	2.13×10^{-2}	8.90×10^{3}	
^{261}Rf	$\left(\frac{3}{2}^+\right)$	0	9.17×10^{-2}	9.84×10^{-2}	
	$\left(\frac{11}{2}^-\right)$	0.100	8.91×10^{-2}	3.44	
^{259}Sg	$\left(\frac{1}{2}^+\right)$	0	8.63×10^{-2}	2.51×10^{-1}	
	$\left(\frac{9}{2}^+\right)$	~ 0	6.83×10^{-2}	2.28×10^{-1}	
^{265}Sg	$\left(\frac{9}{2}^+\right)$	0	8.71×10^{-2}	1.39	
	$\left(\frac{3}{2}^+\right)$	0.070	8.33×10^{-2}	4.85	≈ 17.6

Table 11. Same as the Table 10, but for SF ($T^{\rm sf}_{1/2}$) half-lives.

Nucleus	K^π	E (MeV)	S_α 10^{-2}	$T^{\rm sf}_{1/2}$(th.) (s)	$T^{\rm sf}_{1/2}$(exp.) (s)
^{243}Cm	$\frac{5}{2}^+$	0	5.26	2.57×10^{18}	1.73×10^{19}
	$\frac{1}{2}^+$	0.087	7.42	2.27×10^{12}	
^{249}No	$\left(\frac{7}{2}^+\right)$	0	8.60	57	>19 [25]
	$\left(\frac{1}{2}^+\right)$	0.100	4.96	0.4	
^{251}No	$\left(\frac{7}{2}^+\right)$	0	7.14	346	571 [25]
	$\left(\frac{1}{2}^+\right)$	0.106	8.81	6.6	
^{255}No	$\left(\frac{1}{2}^+\right)$	0	3.33	1.48×10^{4}	
	$\left(\frac{11}{2}^+\right)$	0.270	4.29	3.27×10^{6}	
	$\left(\frac{21}{2}^+\right)$	1.50	2.21	8.77×10^{3}	
^{253}Rf	$\left(\frac{7}{2}^+\right)$	0	4.41	8.6×10^{-3}	$14.6^{+7.0}_{-3.4}\times10^{-3}$ [25]
	$\left(\frac{1}{2}^+\right)$	0			$52.8^{+4.4}_{-4.4}\times10^{-6}$ [26]
	$\left(\frac{1}{2}^+\right)$	0.200	5.23	29.0×10^{-6}	$44^{+17}_{-10}\times10^{-6}$ [25]
	$\left(\frac{7}{2}^+\right)$	0.200			$9.9^{+1.2}_{-1.2}\times10^{-3}$ [26]
^{255}Rf	$\left(\frac{7}{2}^+\right)$	0	6.91	2	2.9
	$\left(\frac{1}{2}^+\right)$	0.140	4.07	2.44×10^{-2}	$>5^{+1.7}_{-1.7}\times10^{-5}$ [27]
^{257}Rf	$\left(\frac{1}{2}^+\right)$	0	8.67	382	338
	$\left(\frac{7}{2}^+\right)$	0.073	1.59	1.07×10^{3}	1.09×10^{3}
	$\left(\frac{21}{2}^+\right)$	1.0832	2.13	270	
^{261}Rf	$\left(\frac{3}{2}^+\right)$	0	9.17	3.2×10^{-2}	
	$\left(\frac{11}{2}^-\right)$	0.100	8.91	6.10	3.17
^{259}Sg	$\left(\frac{1}{2}^+\right)$	0	8.63	1.95	$>1.4\times10^{-3}$
	$\left(\frac{9}{2}^+\right)$	~0	6.83	9.72	8
^{265}Sg	$\left(\frac{9}{2}^+\right)$	0	8.71	872	≥17 [24]
	$\left(\frac{3}{2}^+\right)$	0.070	8.33	42	≈17.6

state (Table 9). For the SHN ^{266}Hs and ^{270}Ds, the predicted half-lives of the isomeric and ground states are almost comparable. Note that the isomer $K=6$ in ^{270}Ds [28] is a possible isomeric state observe in the experiment [29–31].

In even-odd nuclei, the energies of the ground and isomeric states are close and the difference in $T^{sf}_{1/2}$ of these states mainly arises from the difference in K. Accordingly, if K of the isomer is larger than K of the ground state, then $T^{sf}_{1/2}$(isomer)$> T^{sf}_{1/2}$(ground state), that is, the isomeric state is more stable with respect to SF.

The prominent examples of this behavior are found in ^{257,261}Rf (Tables 10, 11). If in this case $T_\gamma > T_{1/2}$(isomer), then the isomer becomes the most stable nuclear state with respect to all decay modes and lives longer than the ground state. In nuclei ^{243}Cm, ^{249,251}No, ^{253,255}Rf, and ^{265}Sg, K(isomer)$< K_{gs}$ and $T^{sf}_{1/2}$(isomer)$< T^{sf}_{1/2}$(ground state) (Table 11).

Since our model describes well the lifetimes of ground and isomeric states with respect to AD and SF, then with this model we can try to extract the spins of isomer and ground state from the experimental values of $T^{\alpha,\mathrm{sf}}_{1/2}$ [32].

7 Summary

The DNS model was developed to describe simultaneously the AD, CR and SF. All these processes were considered as the evolution of the system in the collective coordinates of charge (mass) asymmetry and in the relative distance between the centers of clusters. In contrast to the existing fission models, our model gives the correct absolute values for $T_{1/2}$ of SF, CR, and AD. The DNS model reproduces the global SF and AD isotopic trends for even nuclei U, Pu, Cm, Cf, Fm, No, Rf, Sg, and Hs. In terms of SF (AD) half-lives, the model presented describes well the values which differ up to 34 (20) orders of magnitude. The calculated results for AD and SF from the K-isomeric states of both even-even and even-odd nuclei are consistent with the available experimental data. So, the basic assumption of the model on the collective coordinate which is responsible for the AD, CR, and SF seems to be correct.

As shown for the fissioning even-odd nuclei, the centrifugal potential is strongly affects the shape of the driving potential in the region of asymmetric DNS (especially the DNS with α-particle) increasing the potential energy, for example, the height of the potential barrier, and finally creating the FH. So, within the cluster approach the origin of the SF hindrance is related with the spin dependence of the formation probabilities of the binary cluster configurations which are attributed to the SF. As found, the effect of the inertia parameter on the FH is weaker compared to the effect of potential energy, and the FH is the degree of spin-hindered fission.

For the K-isomers of ^{249,251}No and ^{253,255}Rf, we found that the SF half-lives for isomeric states are smaller than those for the corresponding ground states. As shown, the SF half-life of the $K^\pi = 6^+$ isomer in ^{250}No is comparable with that of the ground state and perhaps with the half-life of internal electromagnetic transition to the ground state. The SF half-lives of the second K-isomers in the nuclei ^{250,252,254}No and ^{254,256}Rf are also predicted. For example, we obtain $T^{\mathrm{sf}}_{1/2} = 1.5$ μs for $K = 16^+$ isomeric state in ^{250}No which is

smaller by about one order of magnitude than the half-life of the ground state. As shown, in ^{254}Rf the isomeric state is more stable against SF than the corresponding ground state. For the SHN ^{266}Hs and ^{270}Ds, the half-lives of the isomeric and ground states are almost comparable.

Acknowledgements

This work was supported by Grant No. 25-42-00018 from the Russian Science Foundation [33].

References

[1] I.S. Rogov, G.G. Adamian, N.V. Antonenko, *Phys. Rev. C* **100** (2019) 024606.
[2] I.S. Rogov, G.G. Adamian, N.V. Antonenko, *Phys. Rev. C* **104** (2021) 034618.
[3] I.S. Rogov, G.G. Adamian, N.V. Antonenko, *Phys. Rev. C* **105** (2022) 034619.
[4] I.S. Rogov, G.G. Adamian, N.V. Antonenko, *Phys. Rev. C* **110** (2024) 014606.
[5] G.G. Adamian, N.V. Antonenko, W. Scheid, In: *Clusters in Nuclei, Vol. 2* (Lect. Notes Phys. **848**), edited by C. Beck (Springer-Verlag, Berlin, 2012) p. 165.
[6] G.G. Adamian, N.V. Antonenko, R.V. Jolos, *Nucl. Phys. A* **584** (1995) 205.
[7] G.G. Adamian et al., *Int. J. Mod. Phys. E* **5** (1996) 191.
[8] J.K. Tuli, *Nuclear Wallet Cards* (BNL, New York, 2000).
[9] F.G. Kondev, M. Wang, W.J. Huang, S. Naimi, G. Audi, *Chin. Phys. C* **45** (2021) 03000001; S. Garg, B. Maheshwari, B. Singh, Y. Sun, A. Goel, A.K. Jain, *At. Data Nucl. Data Tables* **150** (2023) 101546.
[10] P. Jachimowicz, M. Kowal, J. Skalski, *At. Data Nucl. Data Tables* **138** (2021) 101393.
[11] P. Möller, A.J. Sierk, T. Ichikawa, H. Sagawa, *At. Data Nucl. Data Tables* **109-110** (2016) 1.
[12] T.M. Shneidman, G.G. Adamian, N.V. Antonenko, R.V. Jolos, W. Scheid, *Phys. Lett. B* **526** (2002) 322; *Phys. Rev. C* **67** (2003) 014313; G.G. Adamian, N.V. Antonenko, R.V. Jolos, T. M. Shneidman, *Phys. Rev. C* **70** (2004) 064318.
[13] S.N. Kuklin, G.G. Adamian, N.V. Antonenko, *Phys. At. Nucl.* **68** (2005) 1443; *Phys. Rev. C* **71** (2005) 014301; *Phys. At. Nucl.* **71** (2008) 1756; S.N. Kuklin, T.M. Shneidman, G.G. Adamian, N.V. Antonenko, *Eur. Phys. J. A* **48** (2012) 112.
[14] S. Raman et al., *At. Data Nucl. Data Tables* **78** (2001) 1.
[15] http://www.nndc.bnl.gov/nndc/ensdf/. ???
[16] G.G. Adamian, N.V. Antonenko, S.N. Kuklin, B.N. Lu, L.A. Malov, S.-G. Zhou, *Phys. Rev. C* **84** (2011) 024324.
[17] H.L. Hall et al., *Phys. Rev. C* **39** (1989) 1866.
[18] D. Petersen et al., *Phys. Rev. C* **74** (2006) 014316.
[19] J. Kallunkathariyil et al., *Phys. Rev. C* **101** (2020) 011301(R).
[20] J. Khuyagbaatar et al., *Phys. Rev. C* **106** (2022) 024309.
[21] M.S. Tezekbayeva et al., *Eur. Phys. J. A* **58** (2022) 52.
[22] A. Lopez-Martens et al., *Eur. Phys. J. Web Conf.* **290** (2023) 02027.
[23] J. Khuyagbaatar et al., *Phys. Rev. C* **103** (2021) 064303.

[24] F.P. Hessberger, *Eur. Phys. J. A* **53** (2017) 75.
[25] J. Khuyagbaatar et al., *Phys. Rev. C* **104** (2021) L031303.
[26] A. Lopez-Martens et al., *Phys. Rev. C* **105** (2022) L021306.
[27] P. Mosat et al., *Phys. Rev. C* **101** (2020) 034310.
[28] G.G. Adamian, N.V. Antonenko, W. Scheid, *Phys. Rev. C* **81** (2010) 024320; G.G. Adamian, N.V. Antonenko, S.N. Kuklin, and W. Scheid, *Phys. Rev. C* **82** (2010) 054304.
[29] D. Ackermann, Ch. Theisen, *Phys. Scripta* **92** (2017) 083002.
[30] F.P. Hessberger, https://arxiv.org/abs/2309.10468 (2023).
[31] D. Ackermann, S. Antalic, F.P. Hessberger, *Eur. Phys. J. Spec. Top.* (2024) https://doi.org/10.1140/epjs/s11734-024-01150-1.
[32] Yu.Ts. Oganessian et al., *Phys. Rev. C* **109** (2024) 054307.
[33] https://rscf.ru/project/25-42-00018/.